

Liquid Exfoliation of Alkyl-Ether Functionalised Layered Metal-Organic Frameworks to Nanosheets

Supplementary Information

Jonathan A. Foster,^a Sebastian Henke,^b Andreas Schneemann,^b Roland A. Fischer^c and Anthony K. Cheetham^c

- a. Department of Chemistry, University of Sheffield, Sheffield, S3 7HF, UK
- b. Lehrstuhl für Anorganische Chemie II, Organometallics & Materials, Ruhr-Universität Bochum, Universitätsstraße 150, 44801 Bochum, Germany
- c. Department of Chemistry, Technical University Munich, Lichtenbergstrasse 4, D-85748 Garching, Germany and Catalysis Research Centre, Technical University Munich, Ernst-Otto-Fischer Strasse 1, 85748 Garching, Germany
- d. Materials Science and Metallurgy, University of Cambridge, 27 Charles Babbage Road, Cambridge, CB3 0FS, UK

Contents

1. General Details.....	2
2. Synthesis of layered MOF frameworks	2
2.1 Synthesis of dicarboxylate linker 1	2
2.2 Synthesis of Cu(1)(DMF).....	3
2.3 Synthesis of Zn(1)(DMF).....	3
2.4 Crystal structure of Zn(1)(DMF).....	3
3. Exfoliation of Cu(1)(DMF) into different solvents	6
3.1 General methods	6
3.2 Tyndal Scattering	6
3.3 X-ray Powder Diffraction	7
3.4 IR Spectroscopy	18
3.5 TGA analysis	18
4. Atomic Force Microscopy	19
5. UV-Vis Studies	22
5.1 Estimation of concentration of nanosheets in suspension.....	22
5.2 Binding Studies	24
6. References.....	27

1. General Details

Commercial solvents and reagents were used without further purification. Synthesis of organic ligands were carried out in dry glassware with a nitrogen overpressure. Solvothermal synthesis of metal-organic frameworks was undertaken using borosilicate vials with Teflon faced rubber lined caps.

NMR spectra were recorded on a Bruker Advance DPX 400 spectrometer. Chemical shifts for ^1H and ^{13}C are reported in ppm on the δ scale; ^1H and ^{13}C chemical shifts were referenced to the residual solvent peak. All coupling constants are reported in Hz. Mass spectra were collected using an Agilent 6530 QTOF LC-MS in positive ionization mode. Elemental analyses were obtained on an Exeter Analytical CE-440 Elemental Analyzer or Elementar vario MICRO cube.

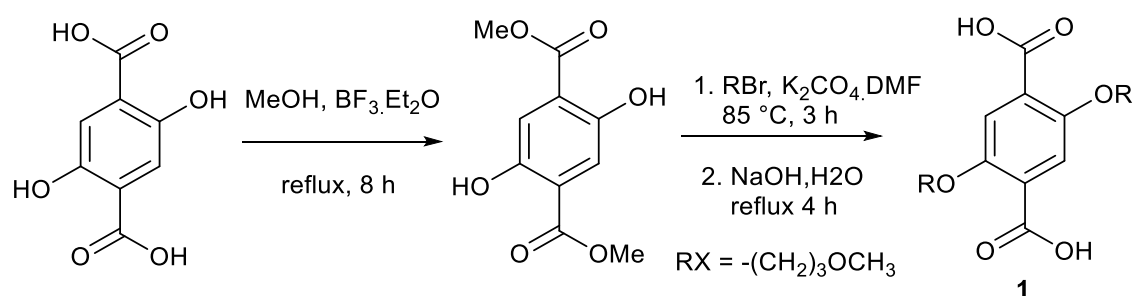
Powder X-ray diffraction data were collected using a Bruker-AXS D8 diffractometer using $\text{CuK}\alpha$ ($\lambda=1.5418 \text{ \AA}$) radiation and a LynxEye position sensitive detector in Bragg Brentano parafocusing geometry using a zero background flat plate sample holder or in transmission using a Kapton capillary. IR spectroscopy was performed on a Perkin Elmer ATR-FTIR Spectrum 2. Thermogravimetric analysis was collected using a Perkin Elmer Pyris 1 TGA from 25-400 $^\circ\text{C}$ at 10 $^\circ\text{C min}^{-1}$.

The nanoscopic morphology of the samples was investigated by atomic force microscopy (AFM) with a Veeco Dimension 3100 microscope operating in tapping-mode using RTESP tips, with a nominally 8 nm end radius. Images were flattened using a second order plane fitting using Gwiddion software.

UV-vis absorption spectra were obtained on a Varian Cary 50 Bio spectrophotometer using standard 1 cm width quartz cells and Perkin Elmer Spectrum One software. Fitting of data and calculation of the binding constants were undertaken using an Excel spreadsheet.

2. Synthesis of layered MOF frameworks

2.1 Synthesis of dicarboxylate linker 1



Dimethyl 2,5-dihydroxyterephthalate, was synthesised according to a previously reported method.[1]

Dimethyl 2,5-dihydroxyterephthalate (1.9064 g, 8.43 mmol) and K_2CO_3 (5.528 g, 40 mmol) were suspended in *N,N*-dimethylformamide (DMF) (70 mL). 1-bromo-3-methoxypropane (2.9616 g, 19.35 mmol) was added dropwise, and the mixture was heated under stirring to 85

°C for 3 h and left for 16 h at RT. The solvent was then filtered and the solute evaporated under reduced pressure at 80 °C. The residue was refluxed in deionised water (90 mL) with NaOH (0.9 g, 10.0 mmol) for 5 h. After cooling to room temperature the solution was acidified with 20 mL aqueous HCl (~15%), and the precipitate was collected by filtration, washed with water (20 mL), and dried in vacuo at 85 °C for 18 h to yield **1** as a peach/yellow powder (2.3210 g, 6.78 mmol, 80 % yield). ¹H NMR (400 MHz, CDCl₃) δ/ppm 11.34 (1H, s, COOH), 7.88 (1H, s, Ar-H), 4.37 (2H, t, *j* = 5.72, OCH₂), 3.63 (2H, t, *j* = 10.73, OCH₂CH₂), 3.37 (3H, s, OCH₃), 2.18 (2H, p, *j* = 5.52, 5.56, CH₂CH₂CH₂). ¹³C NMR{¹H}: 164.34, 151.55, 122.80, 177.03, 70.68, 69.48, 58.92, 29.08. LC-MS (CH₃CN/H₂O): *m/z* 325.1 ([M-H₂O]⁺), 343.1 ([MH]⁺), 365.1 ([M+Na]⁺) Elemental Analysis: analysis calculated for C₁₆H₂₂O₈: Expected: C, 56.14; H, 6.48. Found: C, 55.78; H, 6.37.

2.2 Synthesis of Cu(1)(DMF)

Copper (II) nitrate trihydrate (120.8 mg, 0.5 mmol) and ligand **1** (171.2 mg, 0.5 mmol) were placed into in a 10 mL reaction vial with 10 mL DMF. The vial was sealed and placed in an oven at 110°C for 18 h. After this time, the vial was removed from the oven and allowed to cool to room temperature. The mother liquor was filtered off and the crystals were washed several times with DMF (5 mL) then dichloromethane. Cu(1)·DMF (57.0 mg, 0.14 mmol, 71%) was recovered as a fine green crystalline powder. Elemental analysis: Calculated mass for C₁₉H₂₇CuNO₉ %: C 47.85; H 5.71; N 2.94; Found mass %: C 46.55; H 5.44 N 2.49.

2.3 Synthesis of Zn(1)(DMF)

Zinc (II) nitrate hexahydrate (148.8 mg, 0.5 mmol) and ligand **1** (171.2 mg, 0.5 mmol) were placed into in a 10 mL reaction vial with 10 mL DMF. The vial was sealed and placed in an oven at 110°C for 18 h. After this time, the vial was removed from the oven and allowed to cool to room temperature. The mother liquor was filtered off and the crystals were washed several times with DMF (5 mL) then dichloromethane. Zn(1)(DMF) (57.0 mg, 0.14 mmol, 71%) was recovered as clear prismatic crystals, which were used for single crystal X-ray diffraction.

Elemental analysis of bulk material: Calculated mass for C₁₉H₂₇NO₉Zn %: C 47.66; H 5.68; N 2.93; Found mass %: C 43.30; H 5.13; N 1.68. XRPD analysis (ESI Figure S3) of the bulk material indicates the presence of a second phase which was identified as the previously characterised Zn₄O(1)₃ (a MOF isorecticular to MOF-5, Zn₄O(bdc), with bdc = 1,4-benzenedicarboxylate).

2.4 Crystal structure of Zn(1)(DMF)

A suitable single crystal of Zn(1)(DMF) was selected and mounted on an Oxford Diffraction Xcalibur diffractometer with a Sapphire2 detector. The crystal was kept at 108(2) K during data collection. An empirical absorption correction was applied and the data was integrated and reduced with CrysAlisPro. Using Olex2 [2], the structure was solved with the ShelXS [3] structure solution program using Direct Methods and refined with the ShelXL [4] refinement package using Least Squares minimisation.

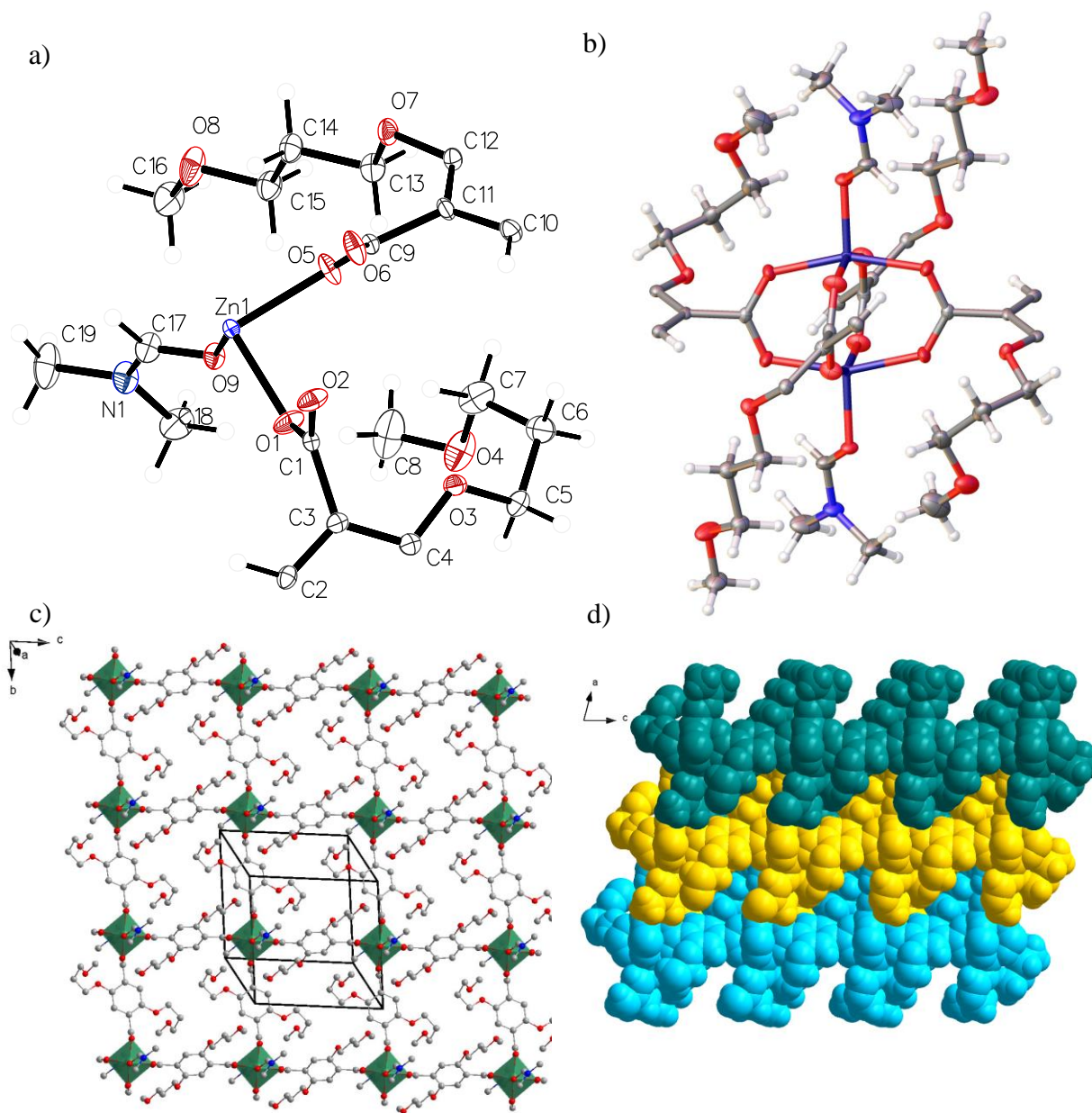


Figure S1: Crystal structure of Zn(1)(DMF): a) labelled ORTEP drawing showing the asymmetric unit b) paddlewheel motif (two asymmetric units), c) view on a single layer. d) Van der Waals space filling model showing stacking between layers.

Table S1 Crystallographic data of Zn(1)(DMF).

Empirical formula	C ₁₉ H ₂₇ NO ₉ Zn
CCDC number	1460747
Formula weight	478.78
Temperature/K	108(2)
Crystal system	triclinic
Space group	<i>P</i> -1
<i>a</i> / Å	10.4273(6)
<i>b</i> / Å	10.8211(5)
<i>c</i> / Å	10.8805(3)
α / °	85.208(3)
β / °	74.992(3)
γ / °	67.508(5)
<i>V</i> / Å ³	1095.45(9)
<i>Z</i>	2
ρ_{calc} / g cm ⁻³	1.452
μ / mm ⁻¹	1.170
F(000)	500.0
Crystal size / mm ³	0.25 × 0.2 × 0.15
Radiation	MoK α (λ = 0.71073)
2 θ range for data collection/°	6.514 to 57.708
Index ranges	-12 ≤ <i>h</i> ≤ 13, -11 ≤ <i>k</i> ≤ 13, -8 ≤ <i>l</i> ≤ 14
Reflections collected	7710
Independent reflections	4844 [R _{int} = 0.0167, R _{sigma} = 0.0423]
Data/restraints/parameters	4844/0/275
Goodness-of-fit on F ²	0.962
Final R indexes [<i>I</i> ≥ 2 σ (<i>I</i>)]	R ₁ = 0.0256, wR ₂ = 0.0550
Final R indexes [all data]	R ₁ = 0.0331, wR ₂ = 0.0558
Largest diff. peak/hole / e Å ⁻³	0.43/-0.26

3. Exfoliation of Cu(1)(DMF) into different solvents

3.1 General methods

In a typical experiment, 10 mg of Cu(1)(DMF) was dispersed in 10 mL of solvent and sonicated using a Fisher Scientific FB15050 Ultrasonic bath (2.75 L, 50 Hz, 80 W) filled with ice cooled water for 30 minutes. The samples were then centrifuged at 1500 rpm for 45 minutes using a Thermo Scientific Heraeus Megafuge 8. The top $\frac{3}{4}$ of the supernatant was decanted into a clean vial and used for the AFM studies of the nanosheets described in section 4 whilst the remaining sediment was used for the majority of XRPD and IR studies described in section 3. Multiple suspensions of nanosheets exfoliated into DMF using this method were combined and subjected to further centrifugation at 4000 rpm for 30 minutes in order to deposit the nanosheets, the results of which are shown in Figure S4a. Measurements collected using a Bragg Brentano geometry were prepared by depositing the concentrated suspension onto a zero background plate and allowing it to dry in air. Capillary measurements were made in transmission mode by drawing a concentrated suspension of material into a Kapton capillary using capillary action and blocking either end with vacuum grease to prevent solvent loss.

3.2 Tyndal Scattering

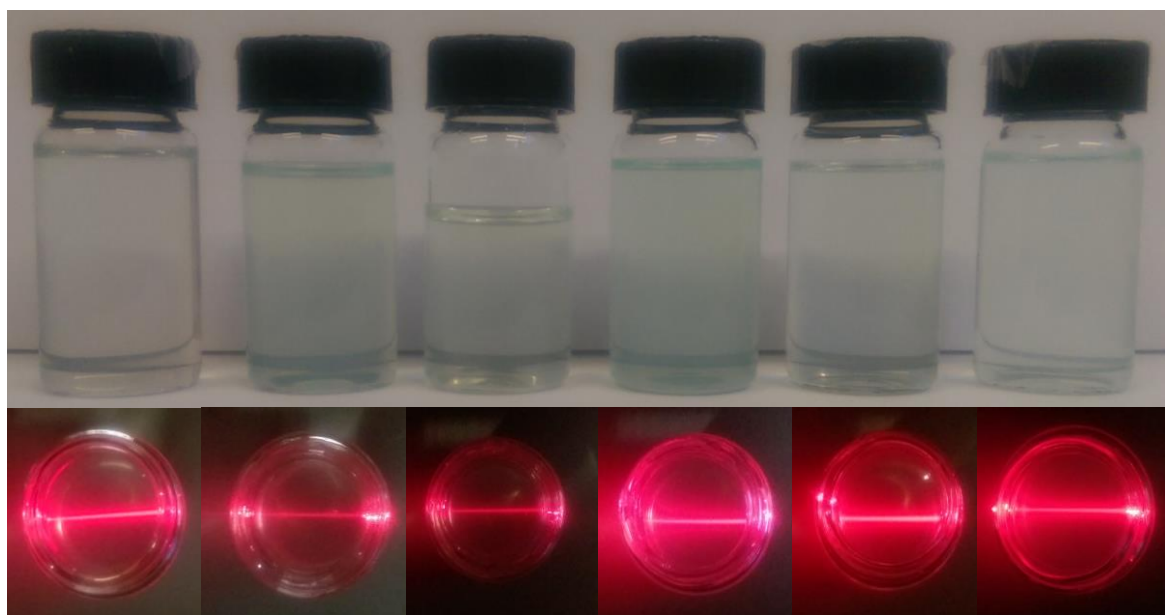


Figure S2: Images showing Tyndal scattering of a suspension of nanosheets exfoliated from Cu(1)(DMF) into (left to right) DMF, 1:1 DMF:Water, water, ethanol, acetone, acetonitrile.

3.3 X-ray Powder Diffraction

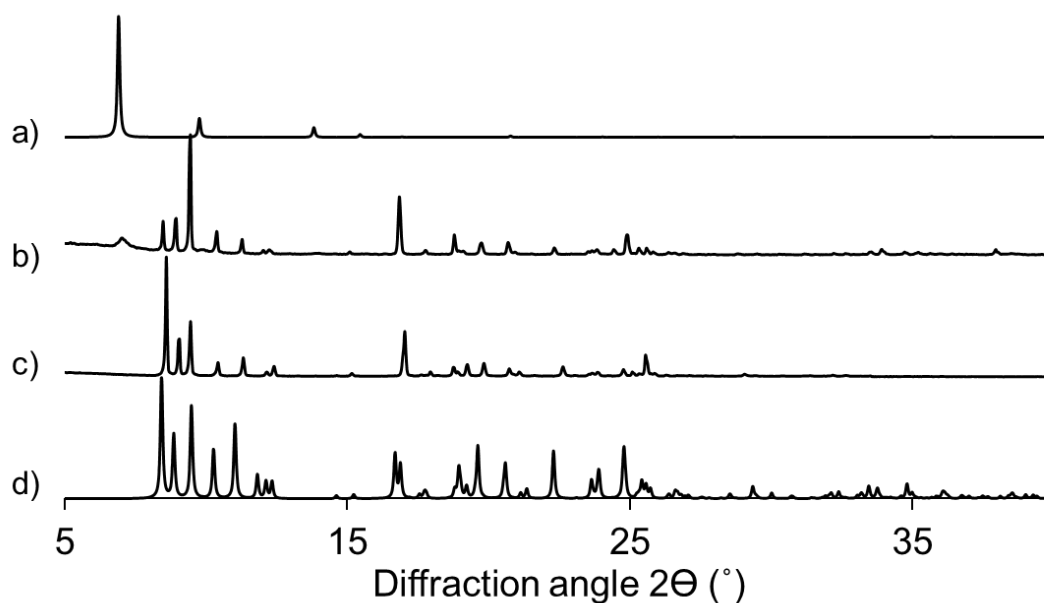


Figure S3: XRPD patterns showing a) the calculated pattern for previously reported [5] $\text{Zn}_4\text{O(1)}_3$ b) the bulk powder pattern for Cu(1)(DMF) , c) the bulk powder pattern for Zn(1)(DMF) , d) calculated pattern for the single crystal structure of Zn(1)(DMF) .

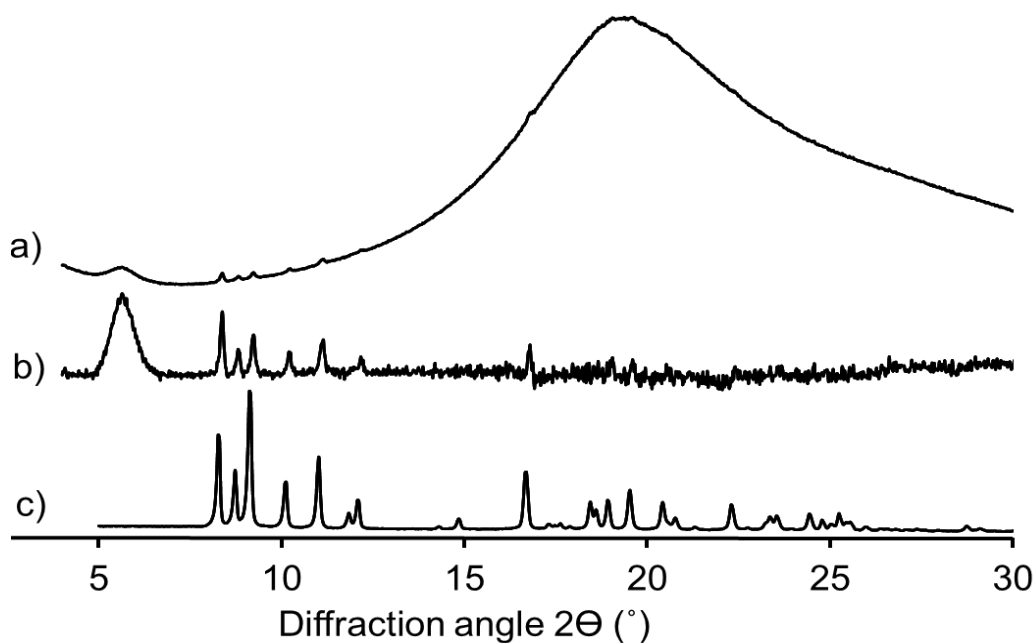


Figure S4: XRPD powder patterns showing a) nanosheets of Cu(1)(DMF) exfoliated in DMF then deposited by centrifugation at 4000 rpm and analysed using a Kapton capillary, b) the same pattern following background subtraction (the broad peak at about 6° 2θ originates from the Kapton capillary and c) an XRPD pattern of the bulk Cu(1)(DMF) deposited following centrifugation at 1500 rpm collected using a flat plate geometry.

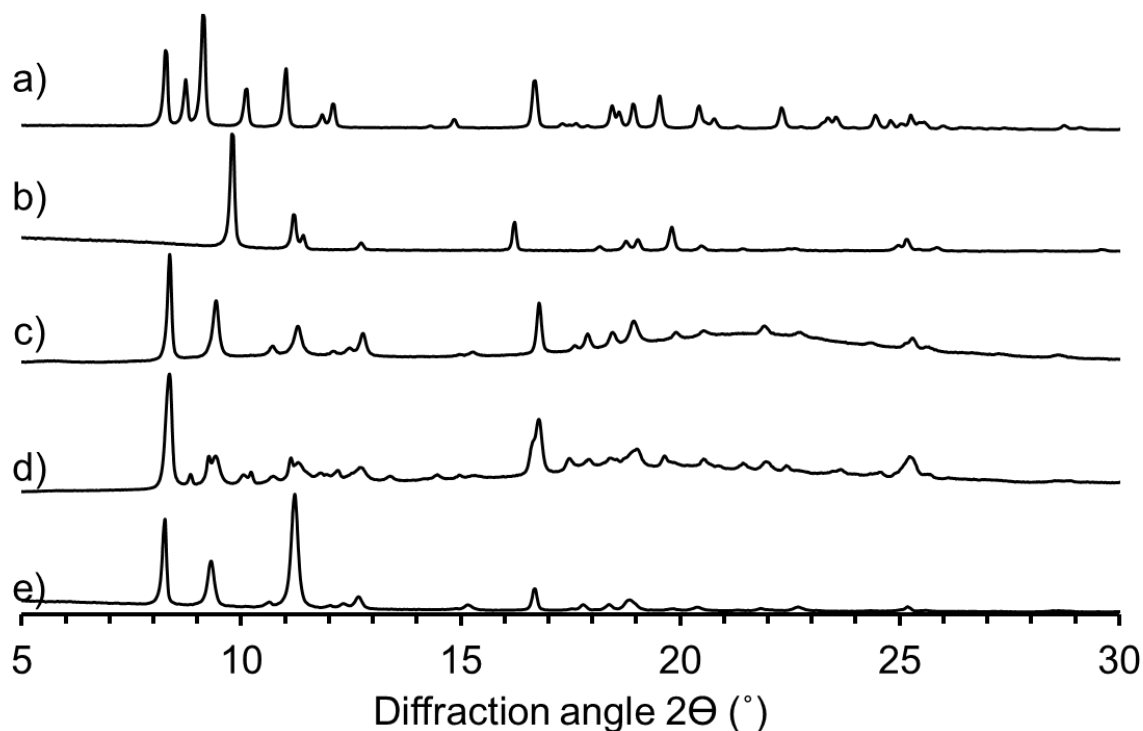


Figure S5: XRPD patterns for Cu(1) derivatives collected by centrifugation from different solvents a) DMF, b) water, c) ethanol,* d) acetone* and e) acetonitrile. Patterns marked with an * were collected using a Kapton capillary with other patterns recorded with a flat substrate and have not been corrected for zero offset.

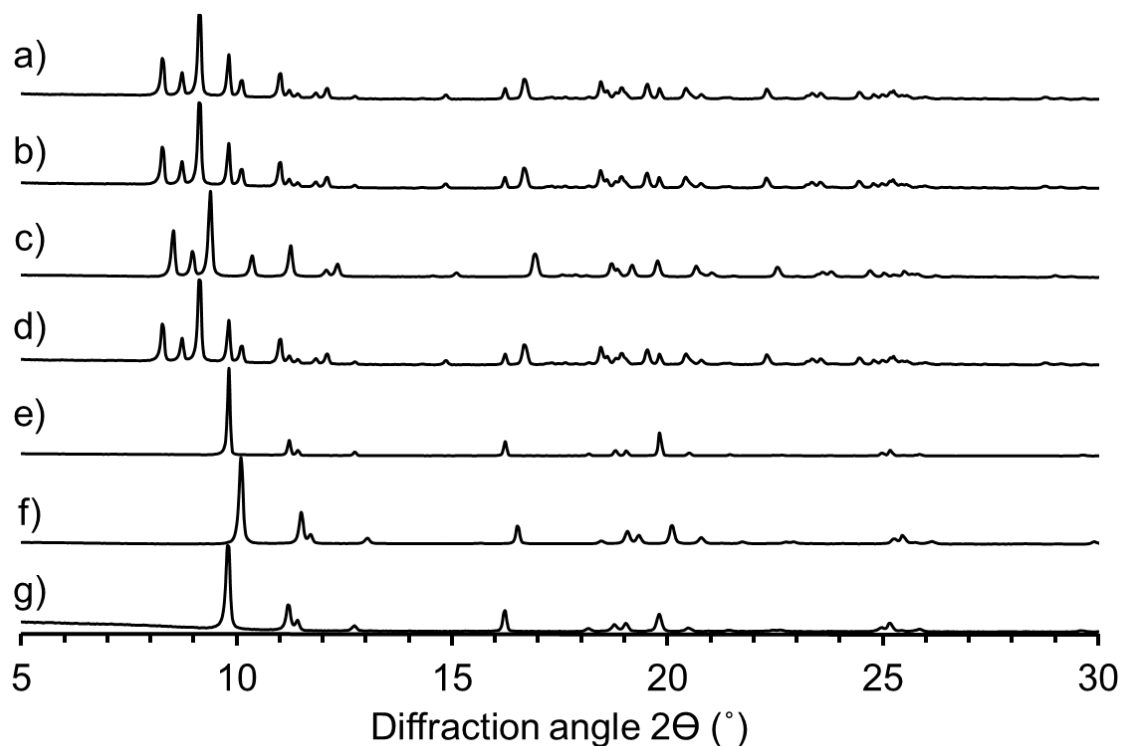


Figure S6: XRPD patterns for Cu(1) derivatives collected by centrifugation from DMF:water mixtures a) 100%, b) 50%, c) 25%, d) 10%, e) 5%, f) 1%, g) 0% DMF. The patterns have not been corrected for zero offset.

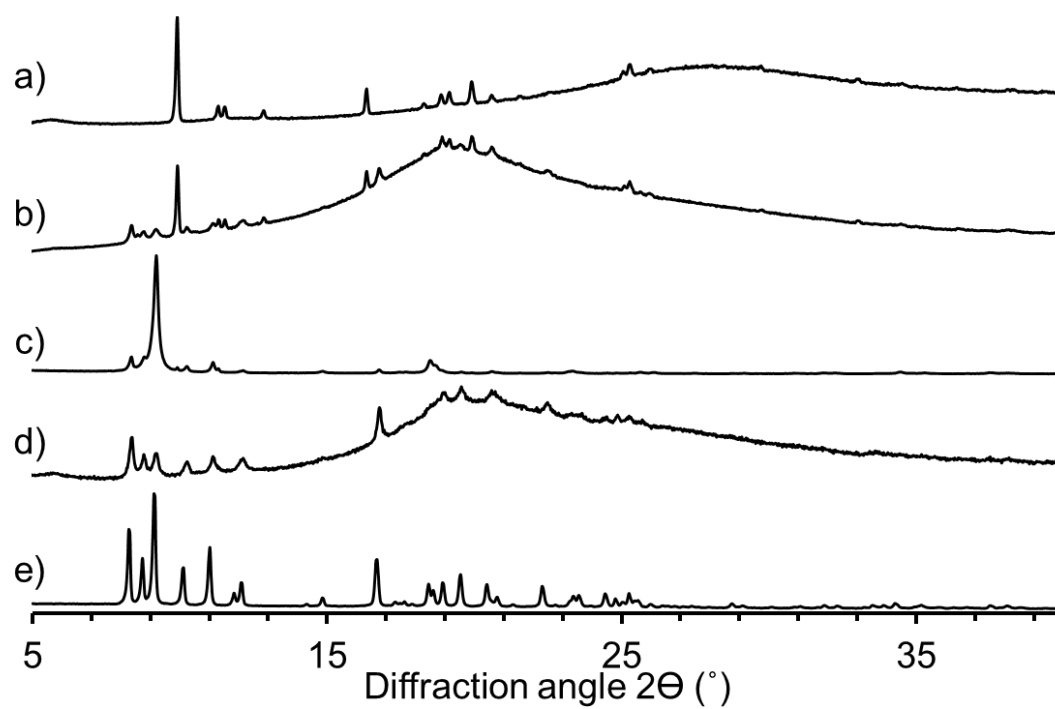


Figure S7: XRPD patterns for Cu(1)(DMF) exfoliated into a) water then recovered and re-immersed in DMF for b) 30 minutes, c) 18 h, d) 4 days with DMF being exchanged twice. e) Cu(1)(DMF) reference pattern.

Table S2 Crystallographic data of the Cu(1)-*solv* materials after immersion in different solvents or X% solvent in water mixtures determined by Pawley refinement of XRPD data.

Sample	Cu(1)-DMF	Cu(1)-50%DMF	Cu(1)-25%DMF	Cu(1)-10%DMF		Cu(1)-5%DMF	Cu(1)-1%DMF	Cu(1)-H ₂ O
				Phase 1	Phase 2			
Suggested formula	Cu(1)(DMF)	Cu(1)(DMF)	Cu(1)(DMF)	Cu(1)(DMF)	Cu(1)(H ₂ O)	Cu(1)(H ₂ O)	Cu(1)(H ₂ O)	Cu(1)(H ₂ O)
Space group	<i>P</i> -1	<i>P</i> -1	<i>P</i> -1	<i>P</i> -1	<i>I</i> 4 ₁ <i>cd</i>			
<i>a</i> / Å	10.5245(6)	10.5671(16)	10.5223(6)	10.5236(7)	15.3426(11)	15.3429(5)	15.3410(7)	15.3419(9)
<i>b</i> / Å	10.7624(6)	10.8300(16)	10.7635(6)	10.7626(7)	15.3426(11)	15.3429(5)	15.3410(7)	15.3419(9)
<i>c</i> / Å	10.8072(6)	10.8595(13)	10.8092(6)	10.8083(8)	31.232(4)	31.2504(13)	31.2683(16)	31.260(2)
α / °	85.293(8)	85.337(17)	85.305(6)	85.302(9)	90	90	90	90
β / °	77.110(5)	76.647(15)	77.008(4)	77.024(6)	90	90	90	90
γ / °	68.264(4)	68.176(17)	68.240(4)	68.245(5)	90	90	90	90
<i>V</i> / Å ³	1108.43(12)	1122.5(3)	1107.88(11)	1107.94(15)	7351.8(14)	7356.5(5)	7358.9(8)	7358(1)
Z (suggested)	2	2	2	2	16	16	16	16
<i>R</i> _{wp}	2.898	5.469	3.097	2.968		5.814	4.223	4.231
<i>R</i> _{exp}	1.081	0.907	1.282	1.199		1.726	1.560	2.422

Sample	Cu(1)-acetonitrile	Cu(1)-EtOH	Cu(1)-acetone	
			Phase 1	Phase 2
Suggested formula	Cu(1)	Cu(1)	Cu(1)(DMF)	Cu(1)
Space group	<i>P</i> -1	<i>P</i> -1	<i>P</i> -1	<i>P</i> -1
<i>a</i> / Å	10.144(5)	10.132(3)	10.560(8)	10.117(9)
<i>b</i> / Å	10.760(6)	10.747(3)	10.833(9)	10.749(9)
<i>c</i> / Å	10.846(5)	10.820(3)	10.839(10)	10.870(7)
α / °	82.55(6)	82.37(3)	84.89(6)	82.98(6)
β / °	93.44(4)	93.574(19)	77.15(5)	94.00(5)
γ / °	51.539(17)	51.781(10)	67.28(3)	51.62(3)
<i>V</i> / Å ³	904.0(9)	901.6(5)	1115.1(17)	903.4(13)
Z (suggested)	2	2	2	2
<i>R</i> _{wp}	5.751	2.969	4.026	
<i>R</i> _{exp}	1.699	0.856	0.912	

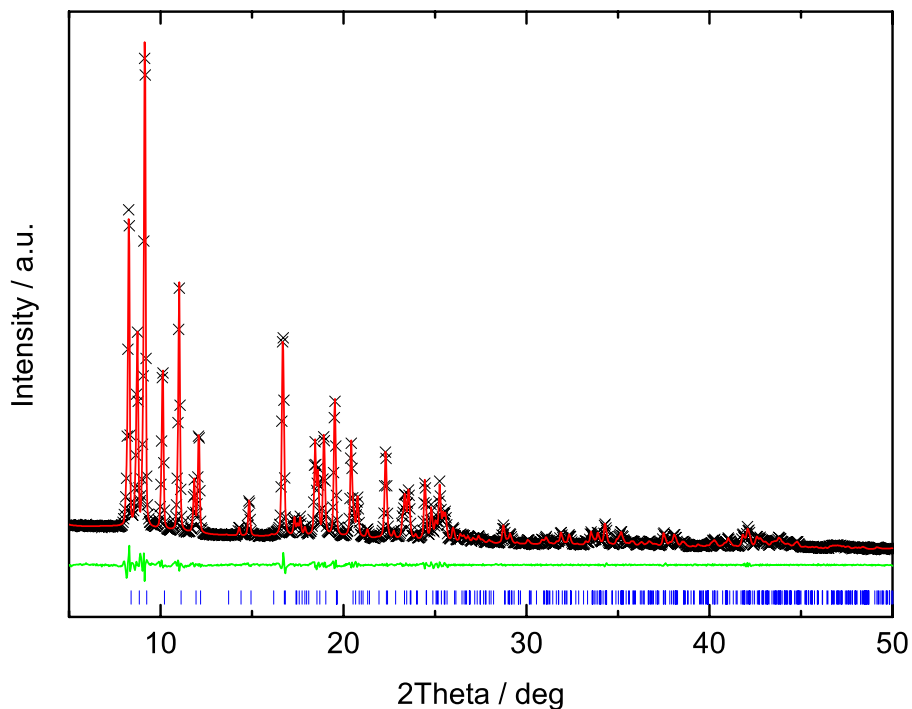


Fig. S8 Pawley fit to the X-ray diffraction pattern of Cu(1)-DMF. The black crosses, red lines, and green lines represent the experimental, calculated, and difference profiles, respectively. The blue tick marks indicate the positions of allowed Bragg reflections in the space group $P-1$.

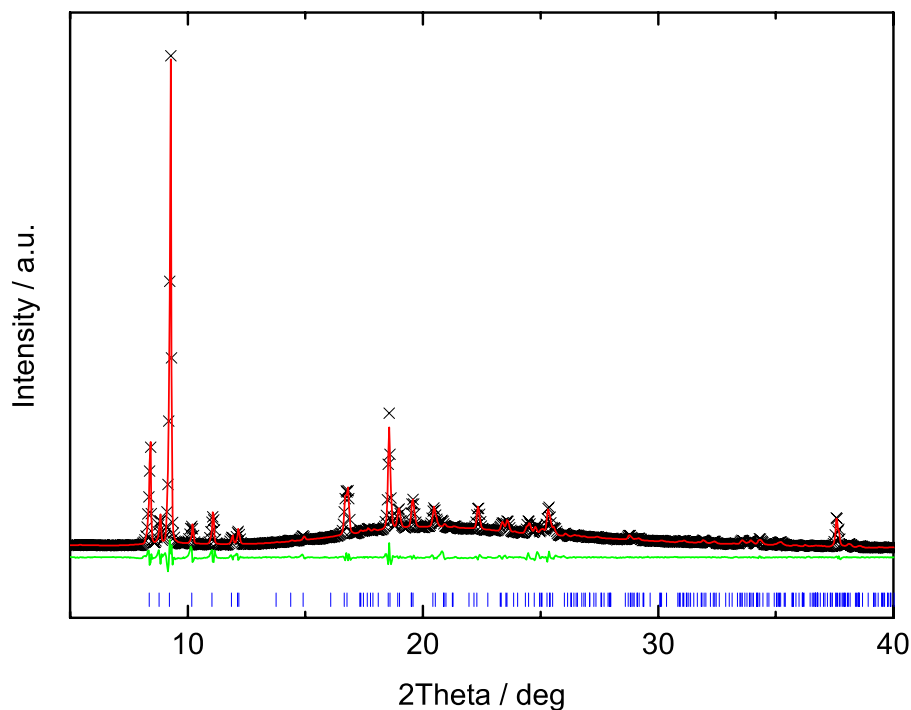


Fig. S9 Pawley fit to the X-ray diffraction pattern of Cu(1)-50%DMF. The black crosses, red lines, and green lines represent the experimental, calculated, and difference profiles, respectively. The blue tick marks indicate the positions of allowed Bragg reflections in the space group $P-1$.

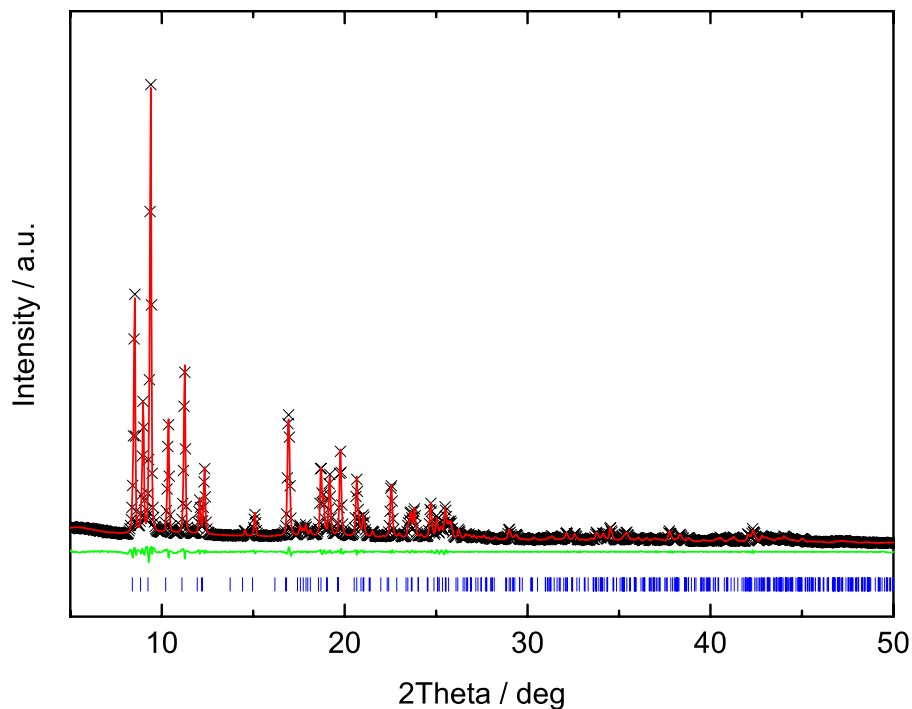


Fig. S10 Pawley fit to the X-ray diffraction pattern of Cu(1)-25%DMF. The black crosses, red lines, and green lines represent the experimental, calculated, and difference profiles, respectively. The blue tick marks indicate the positions of allowed Bragg reflections in the space group $P-1$.

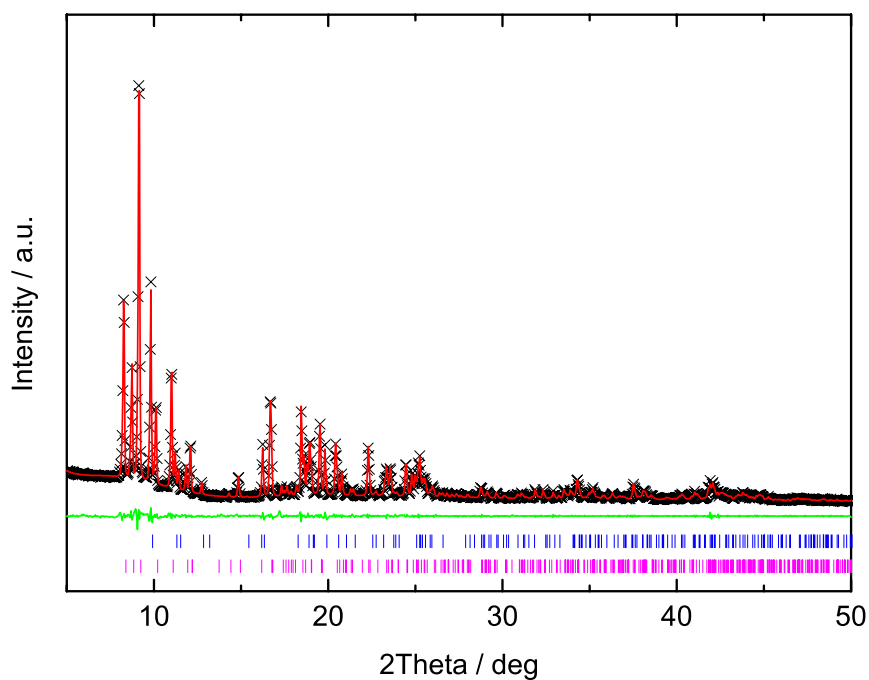


Fig. S11 Two-phase Pawley fit to the X-ray diffraction pattern of Cu(1)-10%DMF. The black crosses, red lines, and green lines represent the experimental, calculated, and difference profiles, respectively. The pink tick marks indicate the positions of allowed Bragg reflections of the DMF phase (Cu(1)(DMF), space group $P-1$) and the blue tick marks indicate the positions of allowed Bragg reflections of the water phase (Cu(1)(H₂O), space group $I4_1cd$).

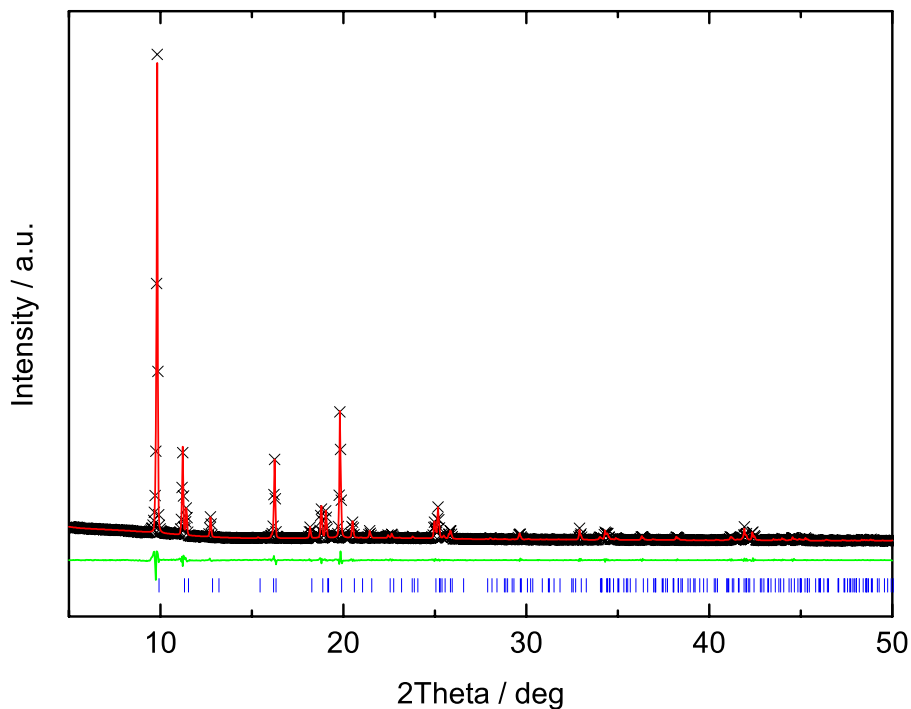


Fig. S12 Pawley fit to the X-ray diffraction pattern of Cu(1)-5%DMF. The black crosses, red lines, and green lines represent the experimental, calculated, and difference profiles, respectively. The blue tick marks indicate the positions of allowed Bragg reflections in the space group $I4_1cd$.

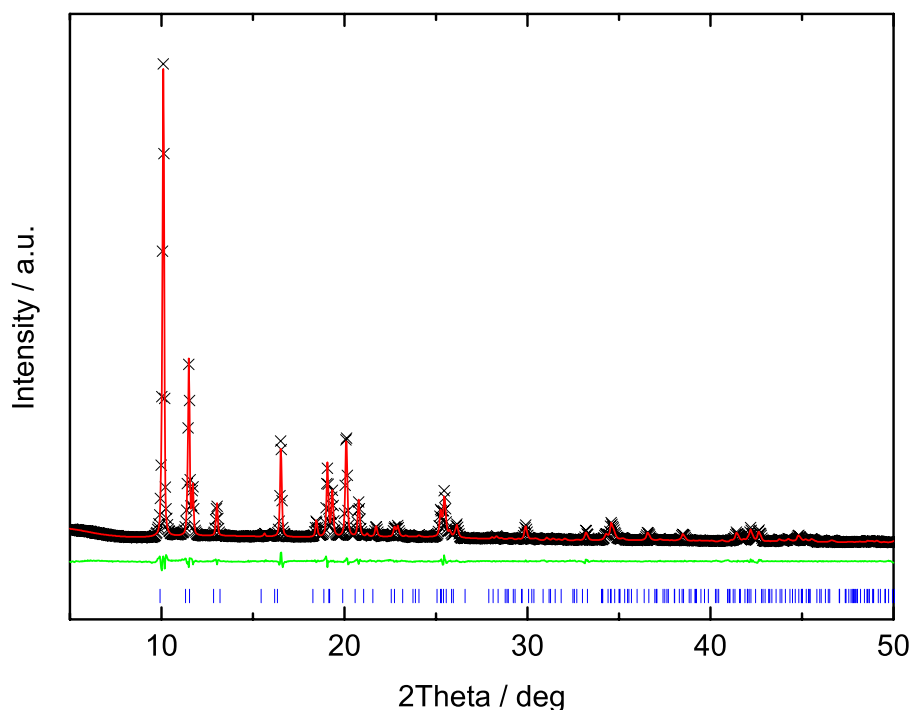


Fig. S13 Pawley fit to the X-ray diffraction pattern of Cu(1)-1%DMF. The black crosses, red lines, and green lines represent the experimental, calculated, and difference profiles, respectively. The blue tick marks indicate the positions of allowed Bragg reflections in the space group $I4_1cd$.

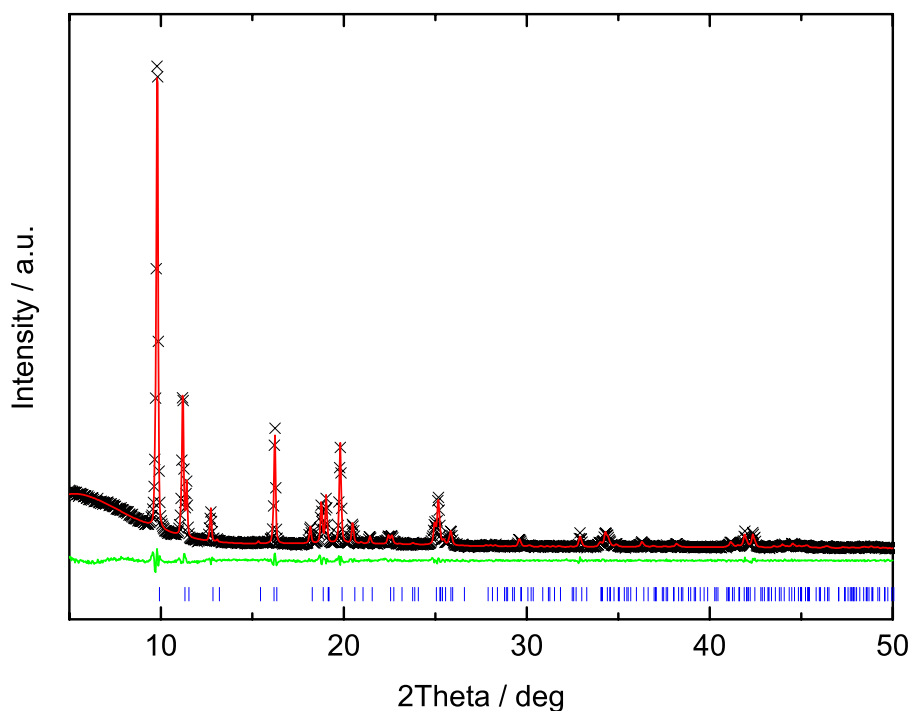


Fig. S14 Pawley fit to the X-ray diffraction pattern of Cu(1)-water. The black crosses, red lines, and green lines represent the experimental, calculated, and difference profiles, respectively. The blue tick marks indicate the positions of allowed Bragg reflections in the space group $I4_1cd$.

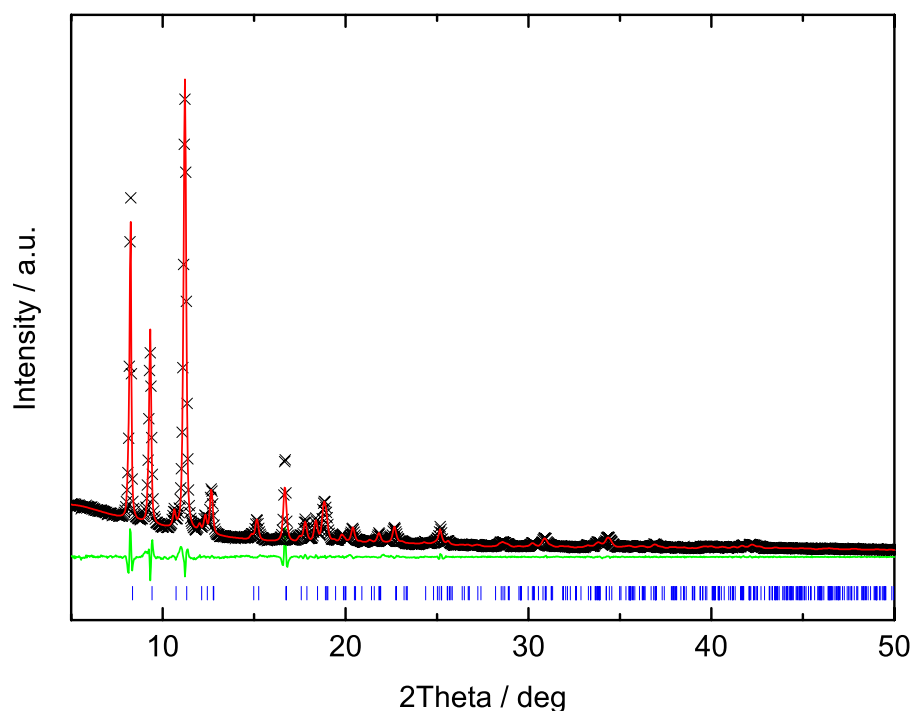


Fig. S15 Pawley fit to the X-ray diffraction pattern of Cu(1)-acetonitrile. The black crosses, red lines, and green lines represent the experimental, calculated, and difference profiles, respectively. The blue tick marks indicate the positions of allowed Bragg reflections in the space group $P-1$.

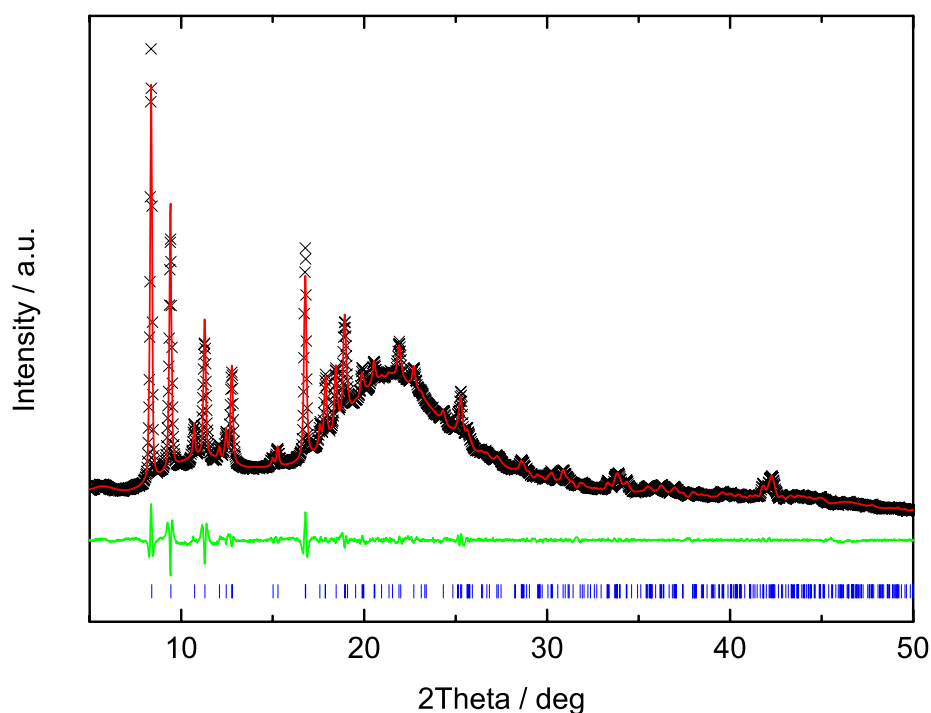


Fig. S16 Pawley fit to the X-ray diffraction pattern of Cu(1)-ethanol (capillary measurement). The black crosses, red lines, and green lines represent the experimental, calculated, and difference profiles, respectively. The blue tick marks indicate the positions of allowed Bragg reflections in the space group $P-1$.

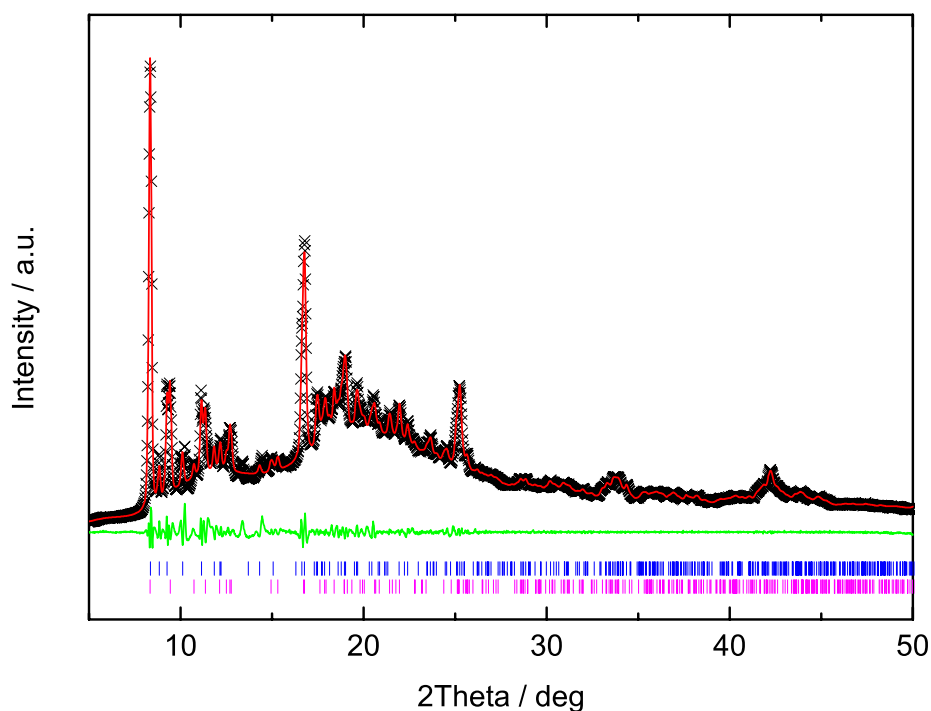


Fig. S17 Two-phase Pawley fit to the X-ray diffraction pattern of Cu(1)-acetone (capillary measurement). The black crosses, red lines, and green lines represent the experimental, calculated, and difference profiles, respectively. The blue tick marks indicate the positions of allowed Bragg reflections Cu(1)(DMF) (space group $P-1$) and the pink tick marks indicate the positions of allowed Bragg reflections of the second phase Cu(1) (also space group $P-1$; unit cell very similar to the material derived from ethanol and acetonitrile).

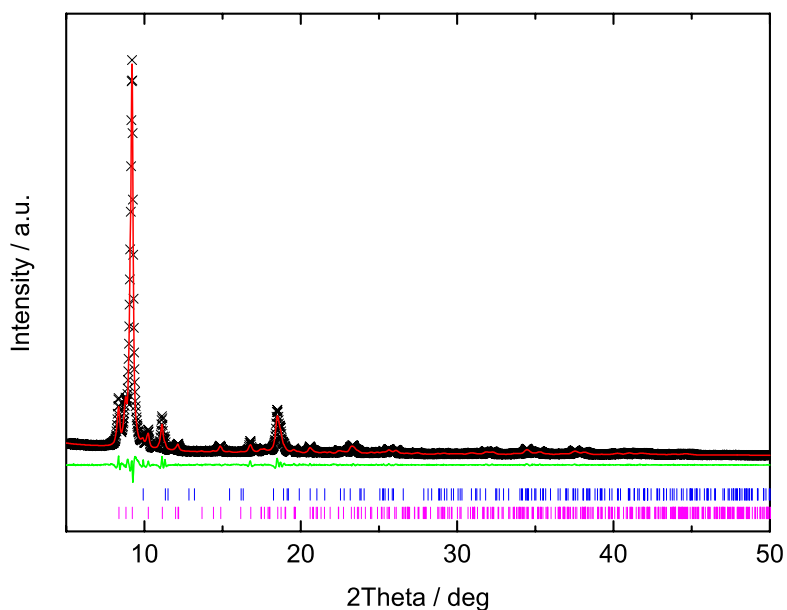


Fig. S18 Two-phase Pawley fit to the diffraction pattern of Cu(**1**) exfoliated in water and then re-immersed in DMF for 18 h. The black crosses, red lines, and green lines represent the experimental, calculated, and difference profiles, respectively. The blue tick marks indicate the positions of allowed Bragg reflections of Cu(**1**)(H₂O) (space group *I4₁cd*) and the pink tick marks indicate the positions of allowed Bragg reflections of Cu(**1**)(DMF) (space group *P-1*). Apparently, the water-containing phase is still the major phase, however, some of the material reverted back to the DMF-containing phase during immersion in DMF. Longer exposure to DMF solvent (4 d), however, results in the complete transformation of Cu(**1**)(H₂O) to Cu(**1**)(DMF) (see Figure S19).

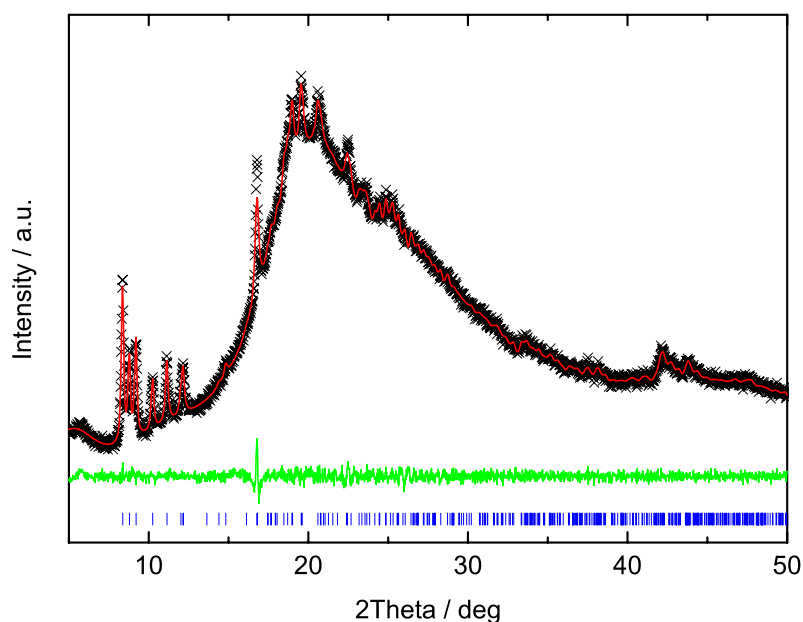


Fig. S19 Pawley fit to the diffraction pattern of Cu(**1**) exfoliated in water and then re-immersed in DMF for 4 d (capillary measurement). The black crosses, red lines, and green lines represent the experimental, calculated, and difference profiles, respectively. The blue tick marks indicate the positions of allowed Bragg reflections of Cu(**1**)(DMF) (space group *P-1*). Apparently, Cu(**1**)(H₂O) has completely reverted to Cu(**1**)(DMF).

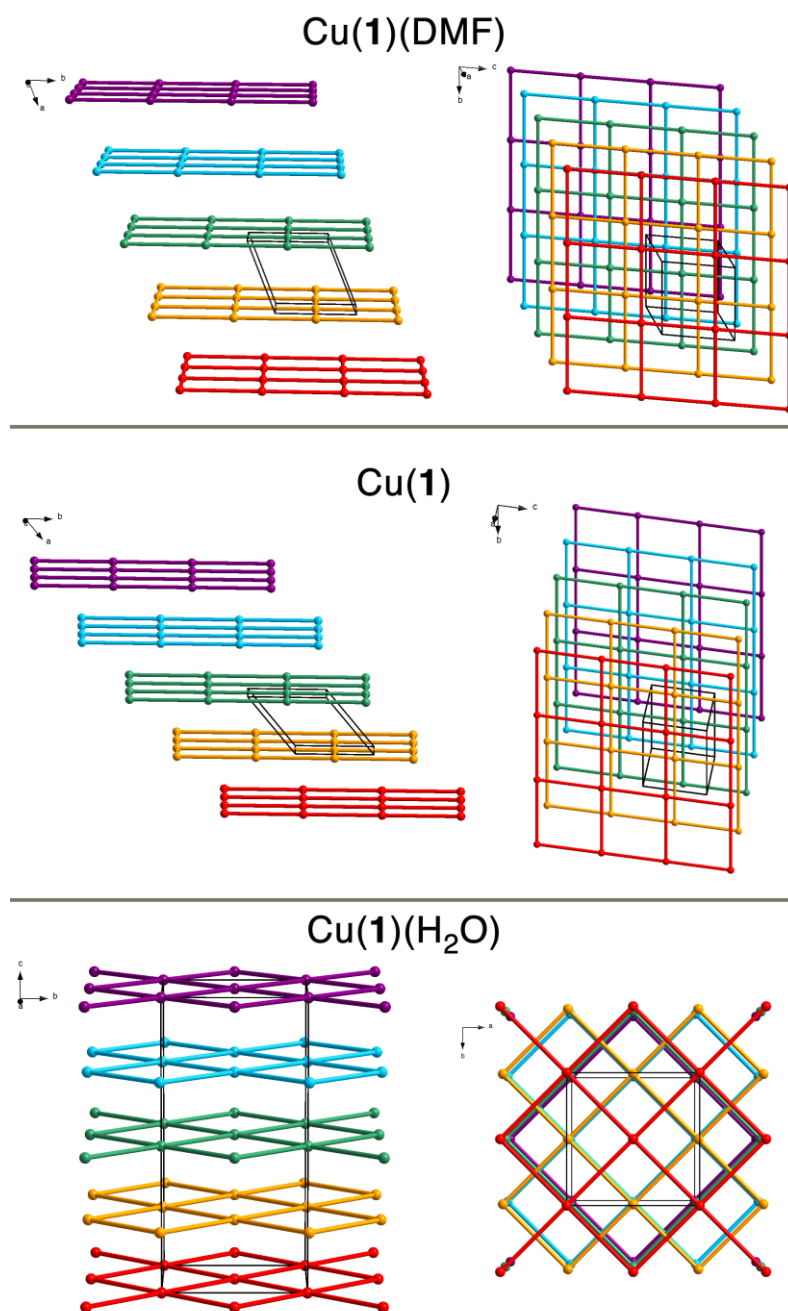


Fig. S20 Representations of the simplified structures of the three different phases of Cu(1) extracted from the Pawley refinement of XRPD data: Cu(1)(DMF) (space group $P-1$), solvent-free Cu(1) (space group $P-1$) and Cu(1)(H₂O) (space group $I4_1cd$). PWs and linkers are represented by spheres and sticks, respectively. Different colours have been used to emphasise neighbouring layers. A side view on the stacked layers is shown on the left and a top view on the stacked layers is shown on the right. Upon removal of DMF the layers move closer together (stacking distance is ~ 7.83 Å in Cu(1) and ~ 9.56 Å in Cu(1)(DMF)). As expected this also results in a reduction of the unit cell volume from 1108 Å³ for Cu(1)(DMF) to 902 Å³ for Cu(1). This reduction corresponds very well to the loss of two DMF molecules per unit cell (approx. 100 Å³ per DMF molecule). Cu(1)(H₂O) exhibits a very different but highly symmetric structure. Neighbouring layers form a staggered arrangement with an interlayer distance of ~ 7.82 Å. The reduced unit cell volume ($2 \cdot V_{\text{unit cell}} / Z$) amounts to 920 Å³, which is in line with the presence of an additional water molecule per formula unit.

3.4 IR Spectroscopy

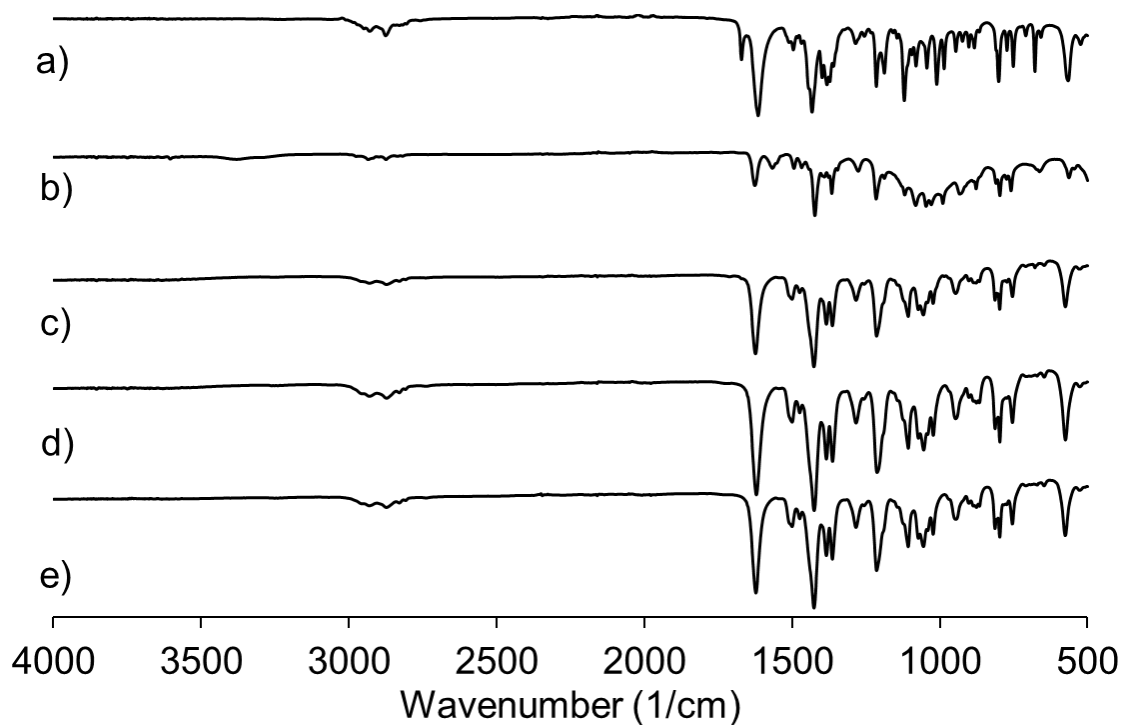


Figure S21: IR patterns for solid collected by centrifugation from different solvents a) DMF, b) water, c) ethanol, d) acetone and e) acetonitrile.

3.5 TGA analysis

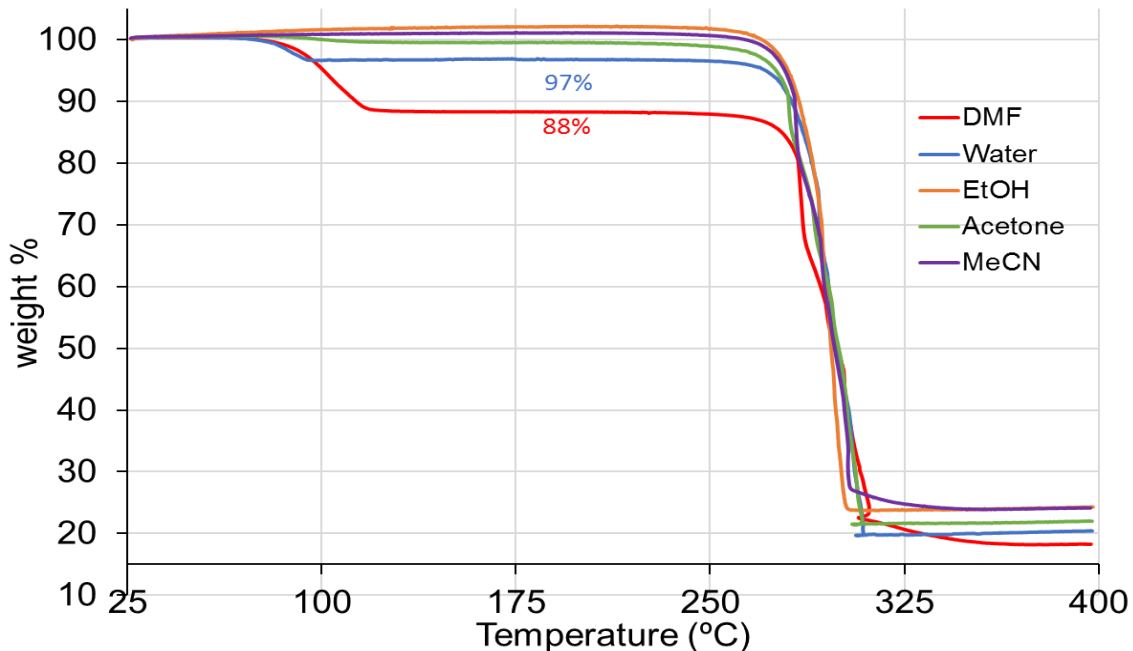


Figure S22: TGA traces showing solvent loss then decomposition of Cu(1) following exfoliation into different solvents. The calculated weight loss upon removal of DMF from Cu(1)(DMF) is 15%. The calculated weight loss upon removal of H₂O from Cu(1)(H₂O) is 4%. 0.5% weight loss is observed from samples exfoliated into acetone, which is attributed to remaining Cu(1)(DMF) phase (as determined by XRPD).

4. Atomic Force Microscopy

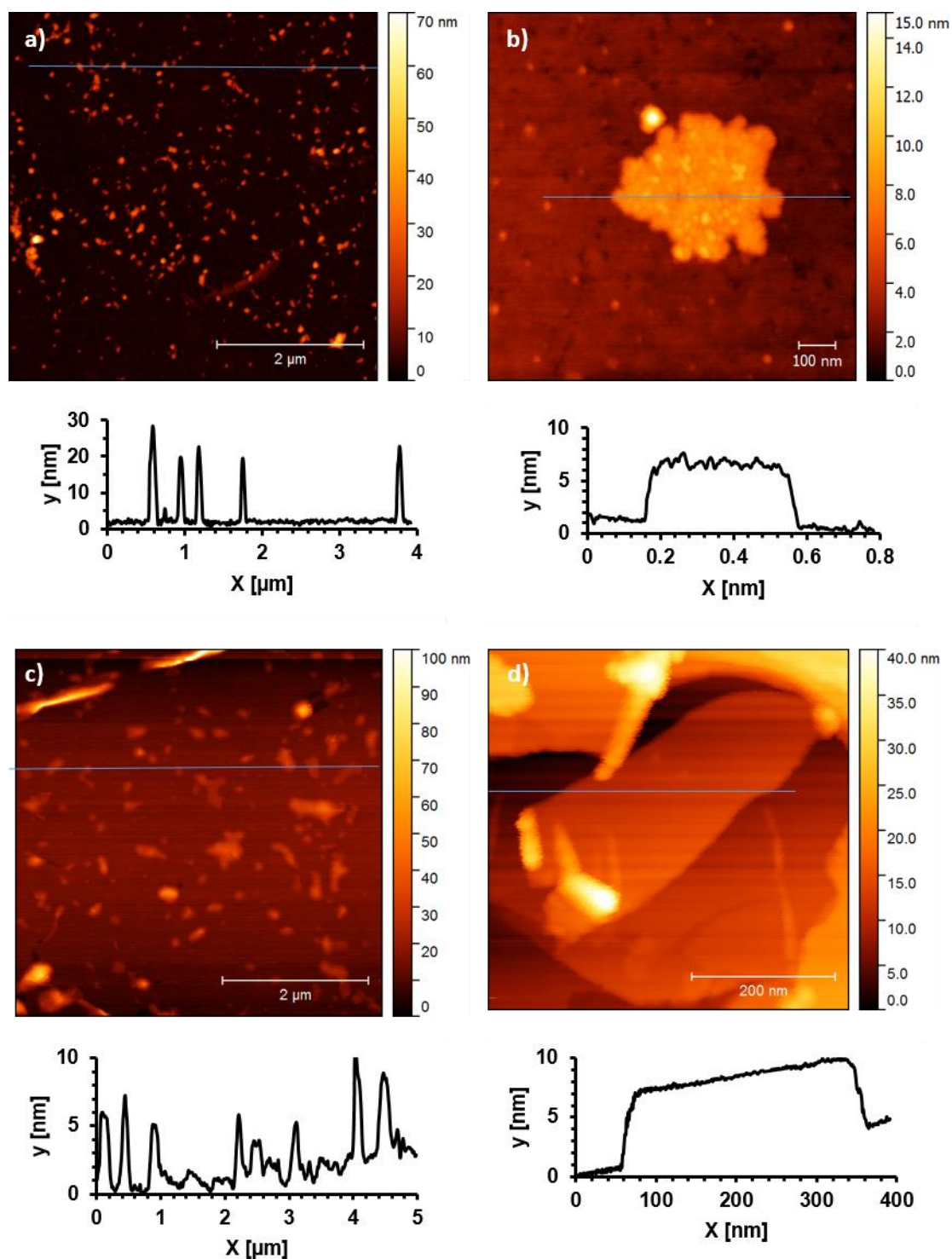


Figure S23, a-d: Tapping-mode AFM images of the delaminated Zn(1)(DMF) nanosheets exfoliated in DMF and deposited on quartz substrates. Height profiles corresponding to the blue lines are shown below each image.

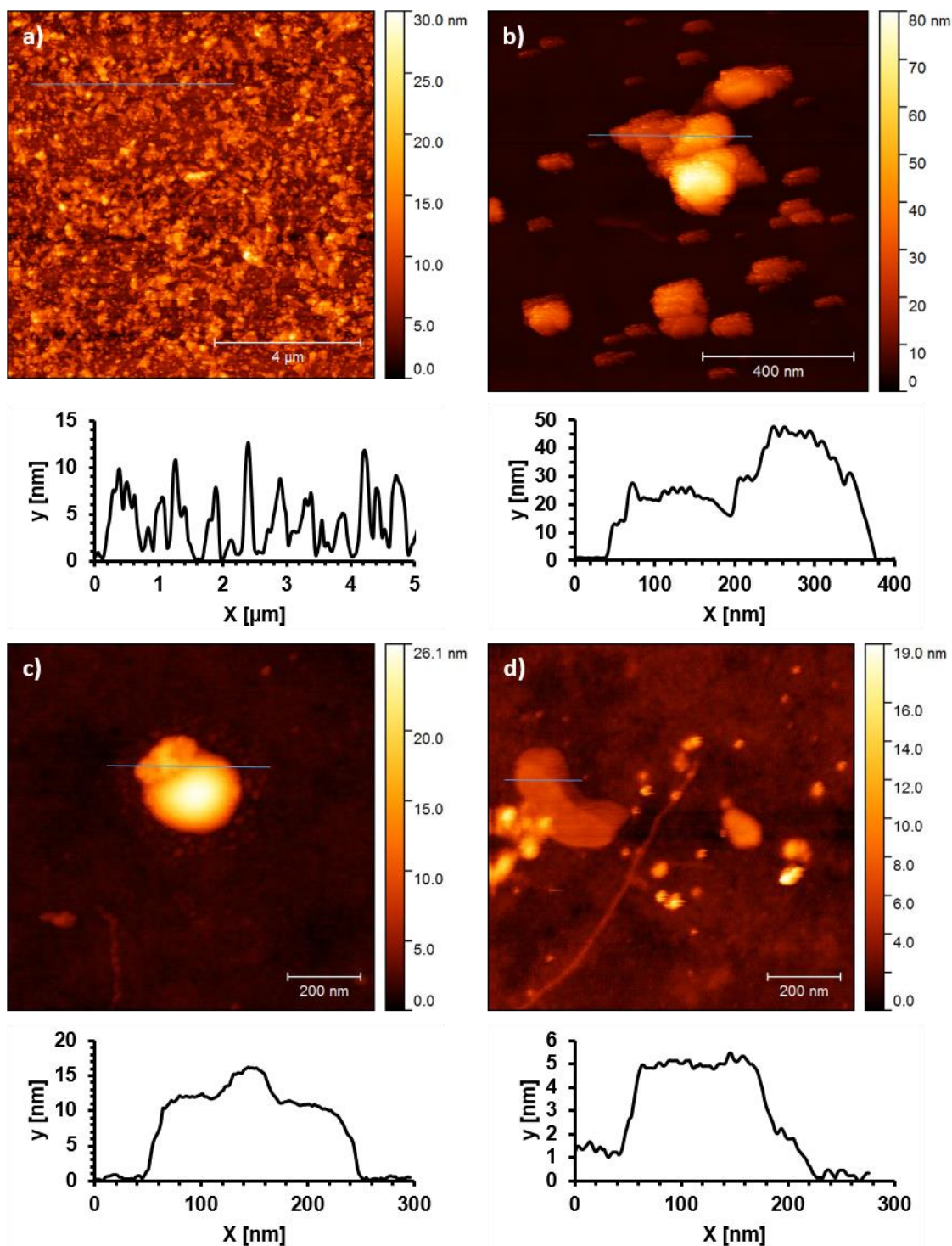


Figure S24, a-d: Tapping-mode AFM images of the delaminated Cu(I)(DMF) nanosheets exfoliated in DMF and deposited on quartz substrates. Height profiles corresponding to the blue lines are shown below each image.

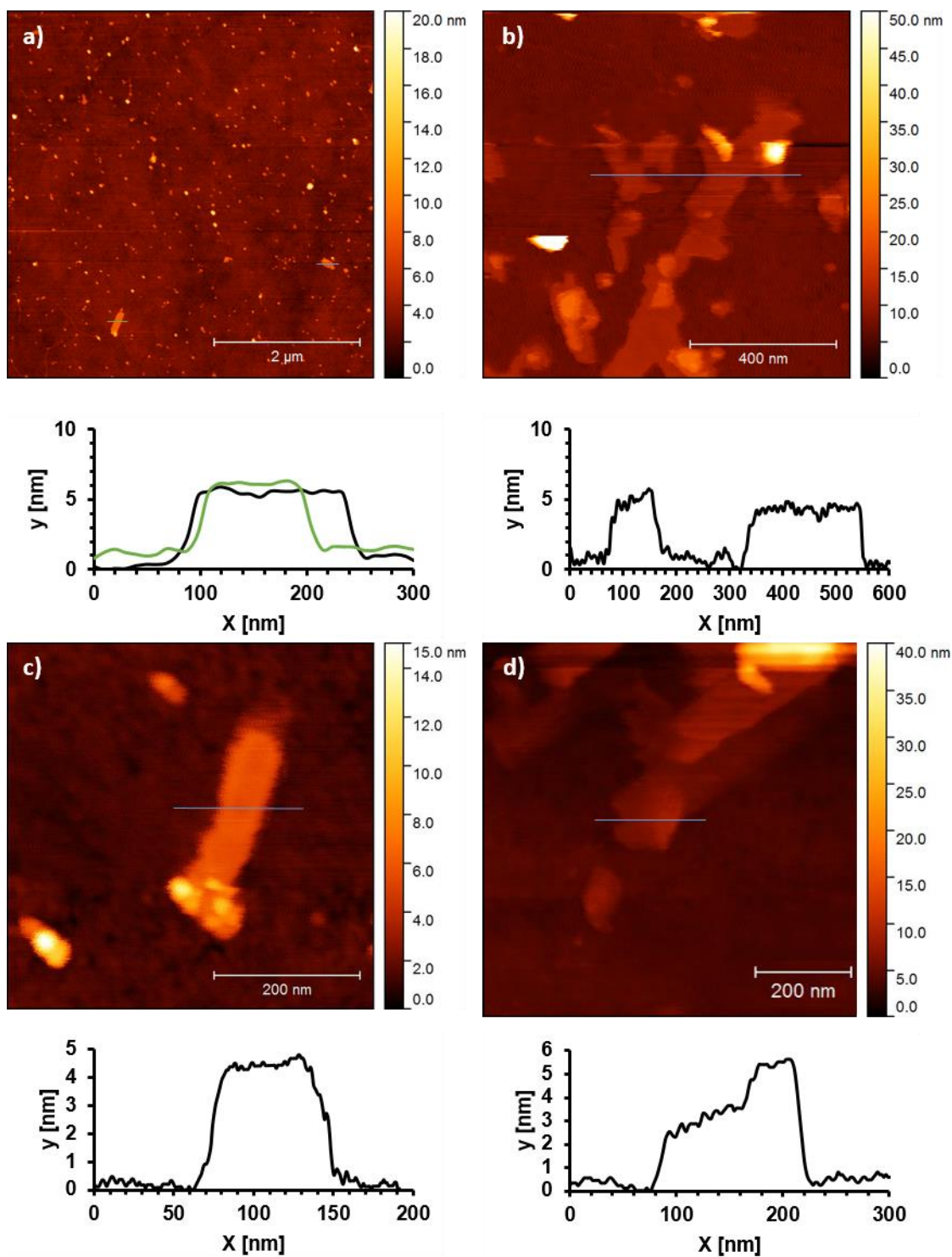


Figure S25, a-d: Tapping-mode AFM images of the delaminated Cu(I)(DMF) nanosheets exfoliated in H₂O and deposited on quartz substrates. Height profiles corresponding to the blue and green lines are shown below each image.

5. UV-Vis Studies

5.1 Estimation of concentration of nanosheets in suspension

The compound was suspended in solvent (1 mg/mL, 2.1 mM) and sonicated in an ultrasound bath for 30 minutes. Aliquots of the uncentrifuged suspension were then titrated into a known volume (2.5 or 3 mL) of solvent in a cuvette with the sample agitated between additions. A calibration curve was generated by plotting concentration against absorbance to determine the extinction coefficient with which the concentration of the suspension can be estimated.

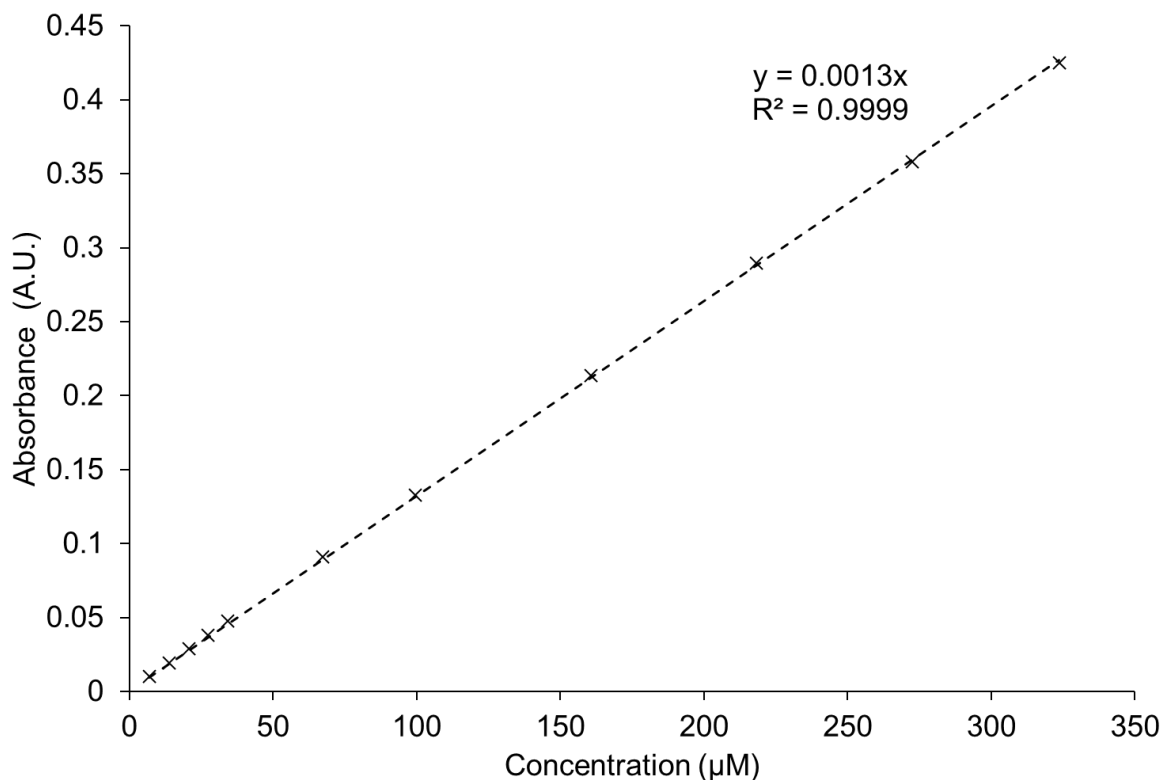


Figure S26: Calibration curve calculating extinction coefficient for Zn(1)(DMF) in DMF measured at $\lambda=310$ nm

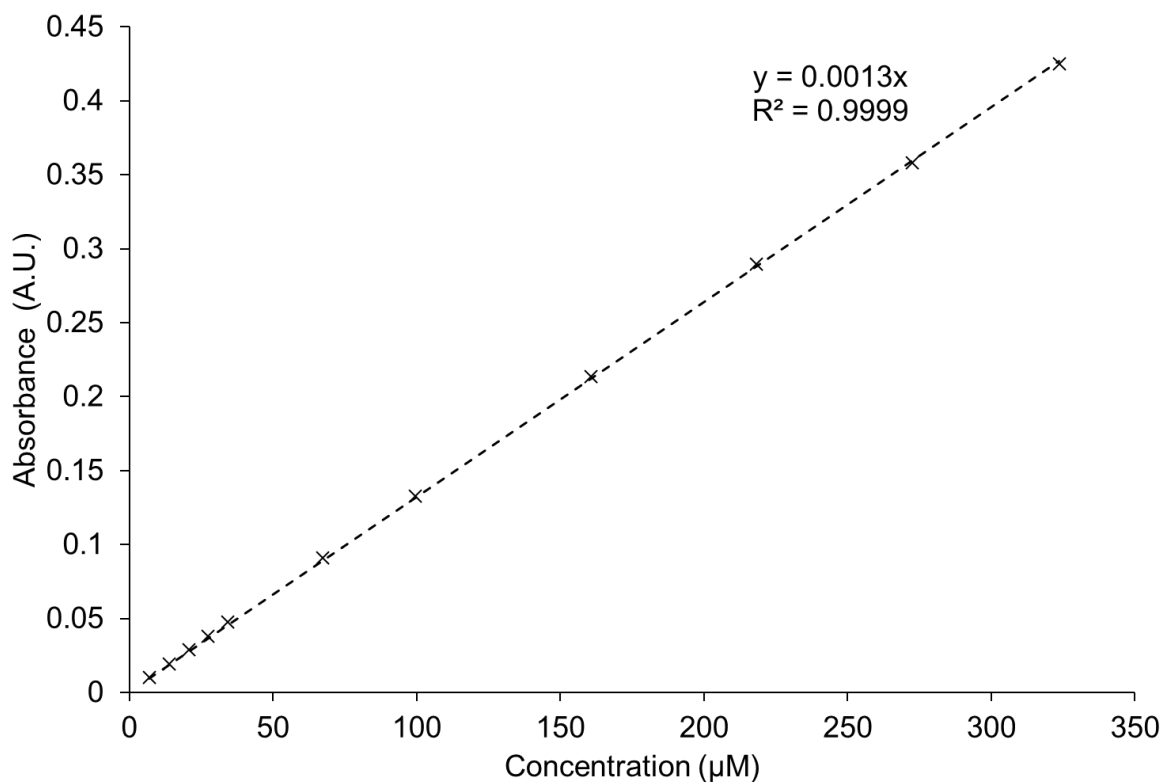


Figure S27: Calibration curve calculating extinction coefficient for Cu(1)(DMF) in DMF at $\lambda_{\text{max}} = 310 \text{ nm}$.

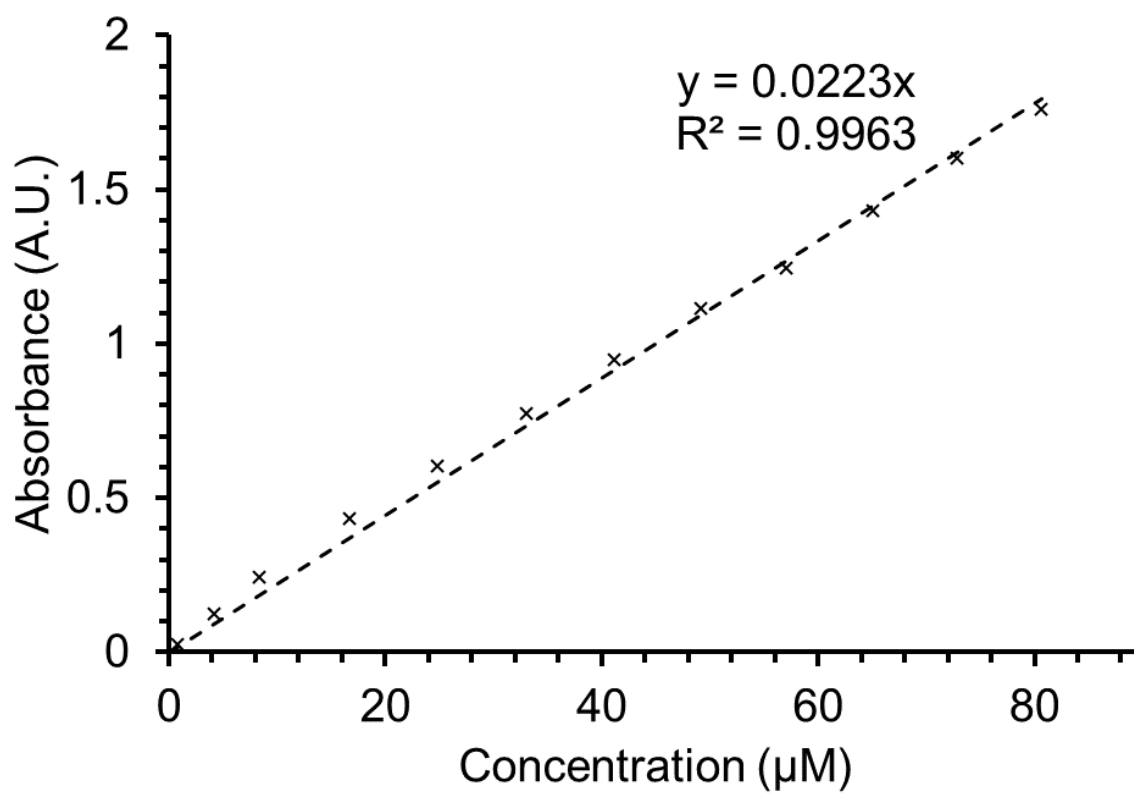


Figure S28: Calibration curve calculating extinction coefficient for Cu(1)(DMF) in water at $\lambda_{\text{max}} = 302 \text{ nm}$.

5.2 Binding Studies

A suspension of the nanosheets was generated by sonicating 10 mg of Cu(1)(DMF) in 10 ml of ice cooled water for 30 minutes before centrifuging the mixture at 1500 rpm for 45 mins. The resulting suspension was diluted with water (1:3) to give a suspension with an absorption maximum at 0.64 AU. Comparison with the calibration curve (Figure S28) indicates this produces a suspension with a concentration of 0.29 mM based on the formula unit of the starting material. Pyridine was dissolved in 5 mL of the host suspension to give a guest solution with a concentration of 1 M. The binding experiments were performed three separate times. Binding constants were obtained by fitting the experimental results to a binding isotherm using 14Allmaster, a macro based excel fitting program written by Christopher A. Hunter (University of Cambridge) and are reported as the global average of the three measurements with the error quoted as two standard deviations from the mean. Tyndal scattering confirmed the presence of nanosheets following addition of pyridine.

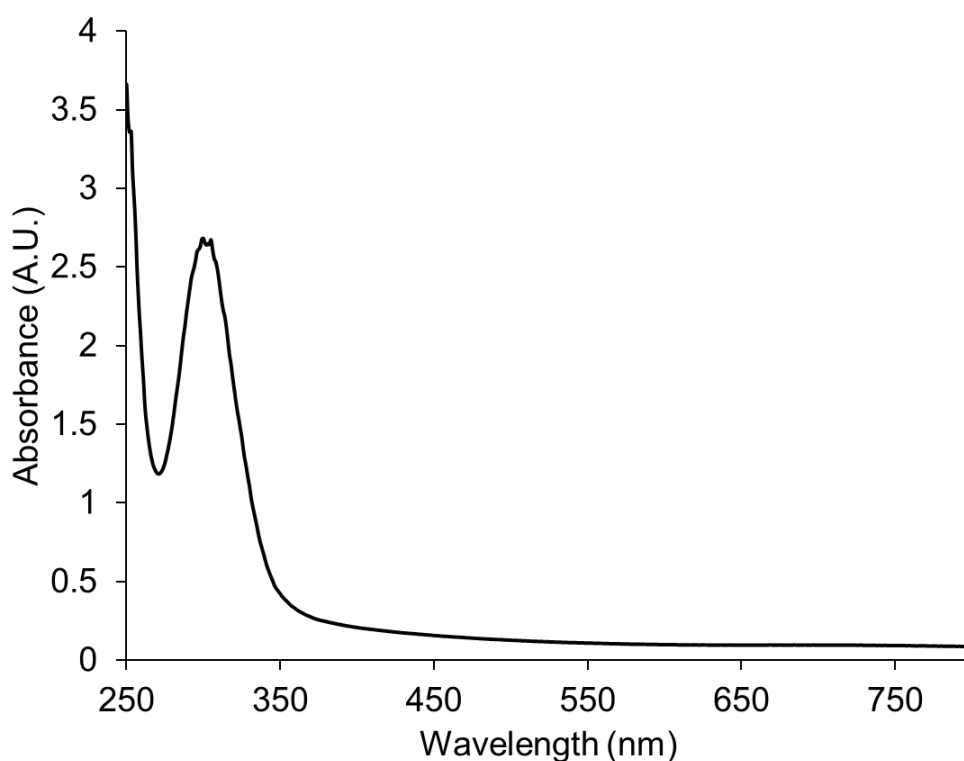


Figure S29: UV-vis spectrum for a suspension of Cu(1) in H₂O (1 mg/ml).

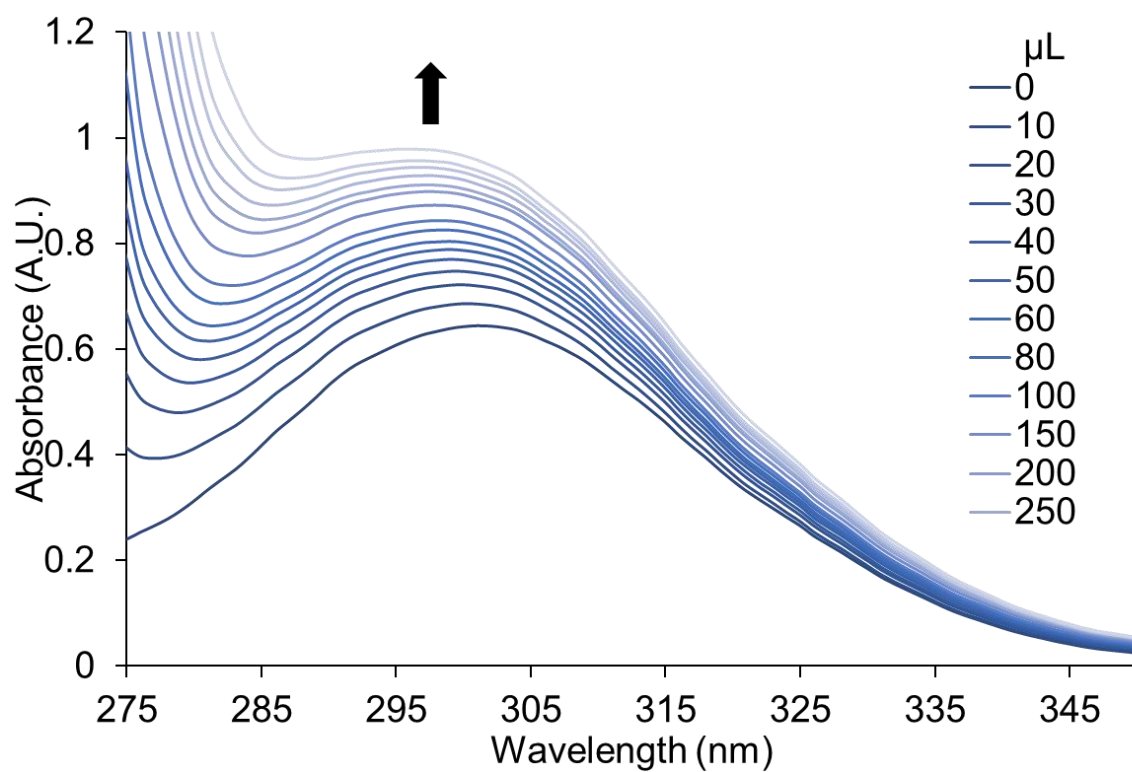


Figure S30: UV-vis plot showing addition of X μL of pyridine solution (1 M in water) to 2.5 mL of an aqueous suspension of Cu(1)(H₂O) nanosheets (0.29 mM).

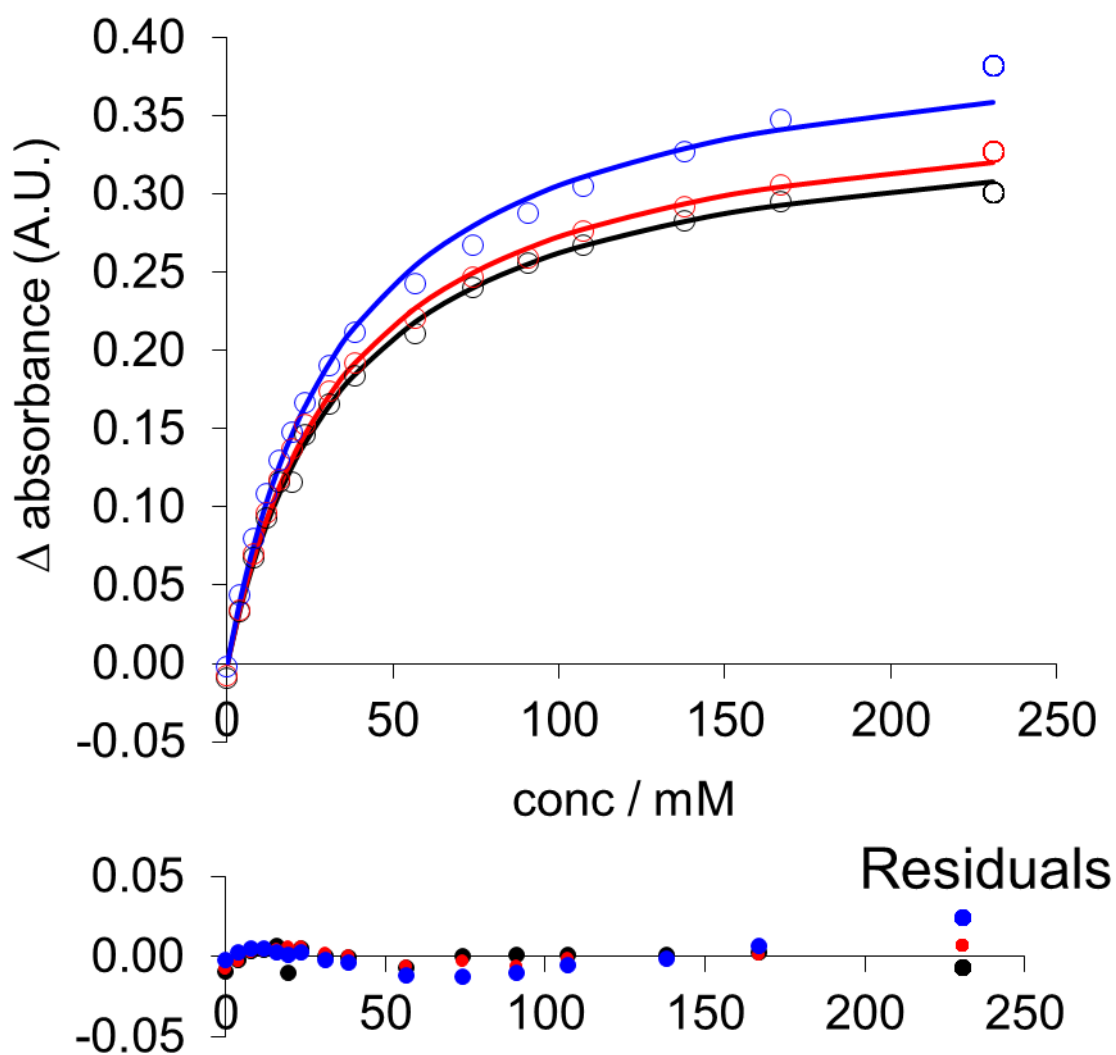


Figure S31: UV-Vis binding titration showing change in absorbance λ_{\max} with changing concentration of pyridine. The experiment was repeated three times with individual experiments shown in red, black and blue. Residuals for fits are shown below.

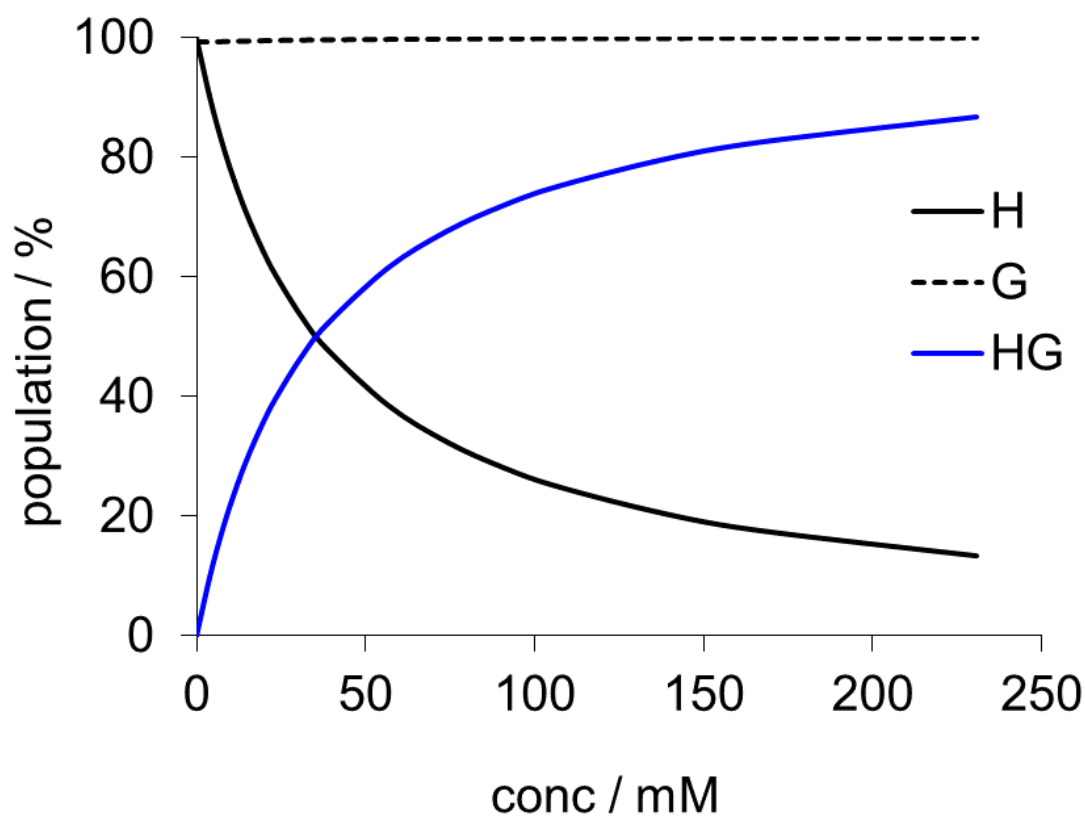


Figure S32: Speciation plot showing formation of HG complex upon addition of pyridine (G) to a suspensions of nanosheets (H).

6. References

1. S. Henke, A. Schneemann, A. Wütscher and R. A. Fischer, *J. Am. Chem. Soc.*, 2012, **134**, 9464.
2. O.V. Dolomanov, L.J. Bourhis, R.J. Gildea, J.A.K Howard, H. Puschmann, *J. Appl. Cryst.*, 2009, **42**, 339.
3. G.M. Sheldrick, *Acta Cryst.*, 2008, **A64**, 112.
4. G.M. Sheldrick, *Acta Cryst.*, 2015, **C71**, 3.
5. S. Henke, R. Schmid, J.-D. Grunwaldt and R. A. Fischer, *Chem. Eur. J.*, 2010, **16**, 14296.